

A Difference Infrared Study of Protein Structural Changes in the Photosynthetic Water-Oxidizing Complex

Jacqueline J. Steenhuis and Bridgette A. Barry*

Contribution from the Department of Biochemistry, University of Minnesota, St. Paul, Minnesota 55108

Received May 20, 1996[⊗]

Abstract: Difference infrared spectroscopy is used to study the manganese-containing catalytic site of photosystem II. Vibrational spectroscopy can test the hypothesis that there are protein conformational differences between the two EPR detectable forms of the S_2 state, which are known as the $g = 4.1$ and the multiline state. A light-minus-dark difference spectrum is constructed at 200, 130, and 80 K. These illumination temperatures generate the S_2 multiline state, the S_2 $g = 4.1$ state, and a chlorophyll cation radical, respectively. Our data show that a unique protein conformation is associated with the formation of the $g = 4.1$ S_2 state. Also, difference infrared spectroscopy demonstrates that formation of the S_2 multiline state perturbs the vibrational spectrum of one or more carboxylic acid residues that may be in the vicinity of the manganese cluster. The perturbation is probably due to a change in hydrogen bonding or effective dielectric constant upon formation of the S_2 state. Further, this carboxylate residue is conserved in plant and in cyanobacterial photosystem II.

Photosynthetic water oxidation occurs at the manganese cluster of photosystem II. Oxidation of water at this site generates molecular oxygen and protons, which contribute to the ATP-producing proton gradient across the chloroplast thylakoid membrane. One-electron photochemistry in the photosystem II reaction center is coupled to the four-electron oxidation of water by accumulation of oxidizing equivalents at the metal cluster. Upon photoexcitation, the manganese cluster cycles through five oxidation states called the S_n states, where n stands for the number of oxidizing equivalents stored. The S_0 state converts to S_1 in the dark by reduction of a stable tyrosine radical, D^{\bullet} . After illumination, there is one spin of D^{\bullet} per reaction center. The S_1 state is stable upon long dark adaptation. The S_4 state is unstable and converts to S_0 with the release of oxygen.¹

The S_2 state can be trapped by continuous illumination at cryogenic temperatures.^{2,3} All S state transitions except S_1 to S_2 are blocked at temperatures below 200 K.³ If a dark-adapted sample in the S_1 state is illuminated at 200 K, the S_2 state that is generated exhibits an EPR signal centered at $g = 2$. This "multiline" signal has at least 16 hyperfine lines with splittings of 87.5 G.⁴ Illumination at 130 K traps an alternate form of the S_2 state with a derivative-shaped EPR signal at $g = 4.1$.^{5–8} While the multiline signal arises from a ground state $S = 1/2$ spin system,⁹ the signal at $g = 4.1$ has been attributed to a $S =$

$5/2$ or $S = 3/2$ spin state.¹⁰ In ammonia-treated samples, hyperfine splittings can be observed on this signal.^{11,12} The $g = 4.1$ signal can be converted to the multiline form by incubation in the dark at 200 K.^{5–7} This process has a negative entropy of activation,¹³ suggesting an ordering of the site is associated with this process. Recent X-ray absorption spectroscopy at the Mn–K edge has shown that there are small structural differences in the cluster when the two forms of the S_2 state are compared.^{14,15} It has been suggested that protein conformational rearrangements may serve to interconvert the two forms of the S_2 state.^{7,8}

Vibrational spectroscopy offers a method with which to test the hypothesis that protein conformational rearrangements underlie the magnetic differences observed between the $g = 4.1$ and multiline states. Difference (light-minus-dark) infrared spectroscopy has been used previously to identify mechanistically important conformational changes in membrane proteins.¹⁶ For this reason, we have obtained difference (S_2 -minus- S_1) infrared spectra on control and $^2\text{H}_2\text{O}$ -exchanged photosystem II complexes at 200 and 130 K.

Materials and Methods

For experiments on plant photosystem II, a monodisperse photosystem II complex preparation¹⁷ with rates of oxygen evolution greater than 1000 μmol of O_2 (mg chlorophyll·h)⁻¹ was employed. The antenna size has been determined to be approximately 120 chlorophylls

* Author to whom correspondence should be addressed.

⊗ Abstract published in *Advance ACS Abstracts*, November 1, 1996.

(1) Debus, R. J. *Biochim. Biophys. Acta* **1992**, *1102*, 269–352.

(2) Brudvig, G. W.; Casey, J. L.; Sauer, K. *Biochim. Biophys. Acta* **1983**, *723*, 366–371.

(3) Styring, S.; Rutherford, A. W. *Biochim. Biophys. Acta* **1988**, *933*, 378–387.

(4) Dismukes, G. C.; Siderer, Y. *Proc. Natl. Acad. Sci. U.S.A.* **1981**, *78*, 274–278.

(5) Casey, J. L.; Sauer, K. *Biochim. Biophys. Acta* **1984**, *767*, 21–28.

(6) Zimmermann, J.-L.; Rutherford, A. W. *Biochim. Biophys. Acta* **1984**, *767*, 160–167.

(7) de Paula, J. C.; Innes, J. B.; Brudvig, G. W. *Biochemistry* **1985**, *24*, 8114–8120.

(8) Zimmermann, J.-L.; Rutherford, A. W. *Biochemistry* **1986**, *25*, 4609–4615.

(9) Dismukes, G. C.; Ferris, K.; Watnick, P. *Photobiochem. Photobiophys.* **1982**, *3*, 243–256.

(10) Reviewed in: Vanngard, T.; Hansson, O. K.; Haddy, A. In *Manganese Redox Enzymes*; Pecoraro, V., Ed.; VCH Publishers: New York, 1992; pp 105–118.

(11) Kim, D. H.; Britt, R. D.; Klein, M. P.; Sauer, K. *J. Am. Chem. Soc.* **1990**, *112*, 9389–9391.

(12) Kim, D. H.; Britt, R. D.; Klein, M. P.; Sauer, K. *Biochemistry* **1992**, *31*, 541–547.

(13) de Paula, J. C.; Beck, W. F.; Miller, A.-F.; Wilson, R. B.; Brudvig, G. W. *J. Chem. Soc.* **1987**, *83*, 3635–3651.

(14) Cole, J.; Yachandra, V. K.; Guiles, R. D.; McDermott, A. E.; Britt, R. D.; Dexheimer, S. L.; Sauer, K.; Klein, M. P. *Biochim. Biophys. Acta* **1987**, *890*, 395–398.

(15) Liang, W.; Latimer, M. J.; Dau, H.; Roelofs, T. A.; Yachandra, V. K.; Sauer, K.; Klein, M. P. *Biochemistry* **1994**, *33*, 4923–4932.

(16) Braiman, M. S.; Rothschild, K. J. *Annu. Rev. Biophys. Biophys. Chem.* **1988**, *17*, 541–570.

(17) MacDonald, G. M.; Barry, B. A. *Biochemistry* **1992**, *31*, 9848–9856.

per reaction center.^{18,19} For some experiments, a photosystem II preparation from the cyanobacterium *Synechocystis* sp. 6803 was used,²⁰ with rates of oxygen evolution of 2200 μmol of O_2 (mg chlorophyll $\cdot\text{h}$)⁻¹. The antenna size of this preparation is approximately 55 chlorophylls per reaction center.^{18,19} Both preparations contain low-potential cytochrome *b*-559.¹⁸ To generate manganese-depleted samples, plant photosystem II preparations were treated with hydroxylamine by a procedure previously described.²¹ For spectroscopic studies, samples contained a stoichiometric amount of potassium ferricyanide (1 mol/mol of reaction center).

Deuterium exchange was performed through concentration and resuspension in a $^2\text{H}_2\text{O}$ buffer or by dialysis. A Centricon-100 concentrating device (Amicon, MA) was employed. The pD is reported as the uncorrected pH meter reading.²¹ In contrast to more rigorous exchange methods,^{21,22} no significant change in the relative intensities of the amide I and amide II bands could be observed in the infrared absorption spectrum after exchange.

Infrared spectra were recorded on a Nicolet 60-SXR spectrometer equipped with a liquid nitrogen-cooled MCT-B detector. Spectral resolution was 4 cm^{-1} , a Happ-Ganzel apodization function was used, double-sided interferograms were collected, mirror velocity was 1.57 cm/s , and 1000 mirror scans were coadded to construct each interferogram. The sample temperature was controlled to ± 0.3 K with a High-Tran liquid nitrogen cryostat (R. G. Hansen & Associates, Santa Barbara, CA) and a temperature control unit (Scientific Instruments model 9620, West Palm Beach, FL). The liquid nitrogen cryostat was equipped with CaF_2 windows. Illumination was provided with a Dolan-Jenner fiber optic annular illuminator equipped with a red filter and a heat filter. A Ge window was used to block any visible or near infrared illumination of the sample from the infrared spectrometer bench. The absorbance of the amide I band at 1655 cm^{-1} was less than 0.9 absorbance unit. The spectra were normalized to an amide II absorbance of 0.5 absorbance unit. To construct the difference spectra, an interferogram recorded under illumination was ratioed directly to an interferogram recorded in the dark. Two to four of these difference spectra were then averaged. Two thousand scans were coadded in some of the experiments performed on $^2\text{H}_2\text{O}$ -exchanged and cyanobacterial samples. Difference spectra obtained with 1000 scans and 2000 scans were identical except for the signal to noise ratio.

EPR control experiments on the production of the S_2 state were performed through the use of a Varian E9 spectrometer equipped with an Air Products cryostat or with a Bruker EMX 6/1 spectrometer equipped with an Oxford cryostat. An EPR spectrum was recorded in the dark before illumination. After illumination at the appropriate temperature, another EPR spectrum was recorded. A light-minus-dark difference spectrum was then generated. Saturating illumination was provided by a Dolan-Jenner fiber optic illuminator equipped with a red filter or with a red and a heat filter. In contrast to a recent report,²³ we have found that illumination of this plant preparation at 130 K gave similar results with and without the heat filter. Samples were illuminated out of the EPR cavity in a transparent, nitrogen-flow dewar. The illumination at 200 K was performed in a dry ice-ethanol bath, the illumination at 130 K was performed by flowing cold nitrogen over the sample, and the illumination at 80 K was performed in a liquid nitrogen bath. Spectra shown in Figure 1 were recorded at 13 K. Spectral conditions were as follows: microwave frequency 9.12 GHz; microwave power 20 mW; modulation amplitude 32 G; scan time 5 min; time constant 0.25 s.

Spin quantitation of photooxidized chlorophyll cation radicals (chl^+) after illumination at 200 and 80 K was performed on a Varian E4 spectrometer equipped with a TE cavity. An EPR spectrum was recorded in the dark before illumination. After illumination at the appropriate temperature, another EPR spectrum was recorded. A light-minus-dark difference spectrum was then generated in which the

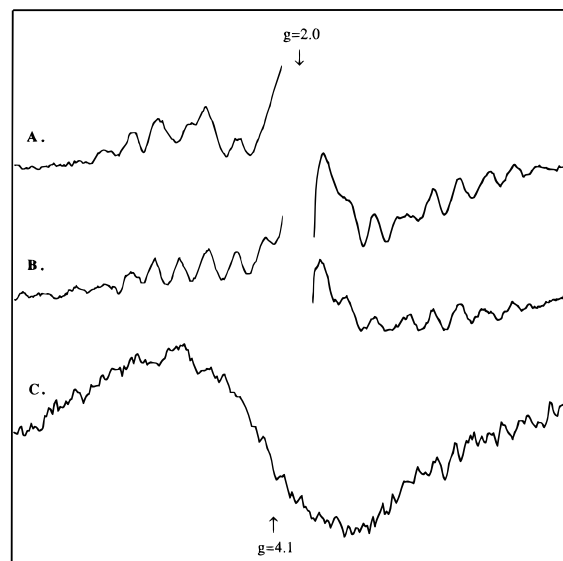


Figure 1. Light-minus-dark difference EPR spectra of (A) cyanobacterial photosystem II illuminated at 200 K, (B) plant photosystem II illuminated at 200 K, and (C) plant photosystem II illuminated at 130 K. The chlorophyll concentration was 1.2 mg chl/mL and the gain was 2.5×10^4 in A. The chlorophyll concentration was 1.7 mg chl/mL, and the gain was 3.2×10^4 in B and C. The spectrum shown in C was expanded by a factor of 3.6 along the y axis and a factor of 1.6 along the x axis for presentation. Spectral conditions are given in the Materials and Methods section.

contributions from the stable tyrosine radical D^{\bullet} were eliminated. The EPR signal in the difference spectrum had a line width of approximately 10 G and was centered at $g = 2.00$. The chlorophyll origin of this signal was suggested previously.^{7,24} Saturating illumination and temperature control out of the EPR cavity were provided as described in the paragraph above. Fremy's salt was used as a spin standard.²⁵ Spectra were recorded at 95 K. Spectral conditions were as follows: microwave frequency 9.1 GHz; microwave power 0.6 mW; modulation amplitude 3.2 G; scan time 4 min; time constant 2.0 s.

Results

In Figure 1, we present light-minus-dark EPR spectra recorded on photosystem II samples that have been illuminated at 200 and 130 K. As expected, illumination of dark-adapted plant photosystem II complexes at 130 K produces mainly the $g = 4.1$ form of the S_2 state (Figure 1C), while illumination at 200 K produces mainly the multiline form of the S_2 state (Figure 1B). At 200 K, a low-amplitude signal at $g = 4.1$ is observed. The intensity of this signal is less than one-half the intensity of the $g = 4.1$ signal observed at 130 K. This behavior is slightly different from previous results, where the signals were shown to interconvert more cleanly.^{7,24} The origin of the difference may be due to the difference in the cryoprotectant employed. However, this effect may also be preparation dependent. The preparation employed in our study is monodisperse, contains low-potential cytochrome *b*-559, and retains the 18 and 24 kDa proteins.¹⁸ Such a preparation has never before been examined with this technique.

Illumination of a cyanobacterial photosystem II preparation at 200 K also produces a multiline signal (Figure 1A). No $g = 4.1$ signal was observed upon illumination of the cyanobacterial preparation at this temperature. A $g = 4.1$ signal has never been observed in a cyanobacterial sample (reviewed in Debus¹).

Illumination of the plant photosystem II samples at 80 K generated a chlorophyll cation radical in a stoichiometry of 0.81

(18) MacDonald, G. M.; Boerner, R. J.; Everly, R. M.; Cramer, W. A.; Debus, R. J.; Barry, B. A. *Biochemistry* **1994**, *33*, 4393–4400.

(19) Patzlaff, J. S.; Barry, B. A. *Biochemistry* **1996**, *35*, 7802–7811.

(20) Barry, B. A. *Methods Enzymol.* **1995**, *258*, 303–318.

(21) Bernard, M. T.; MacDonald, G. M.; Nguyen, A. P.; Debus, R. J.; Barry, B. A. *J. Biol. Chem.* **1995**, *270*, 1589–1594.

(22) Earnest, T. N.; Herzfeld, J.; Rothschild, K. J. *Biophys. J.* **1990**, *58*, 1539–1546.

(23) Boussac, A.; Girerd, J.-J.; Rutherford, A. W. *Biochemistry* **1996**, *35*, 6984–6989.

(24) de Paula, J. C.; Li, P. M.; Miller, A.-F.; Wu, B. W.; Brudvig, G. W. *Biochemistry* **1986**, *25*, 6487–6494.

(25) Wertz, J. E.; Bolton, J. R. *Electron Spin Resonance*; Chapman and Hall: London, 1986; pp 462–463.

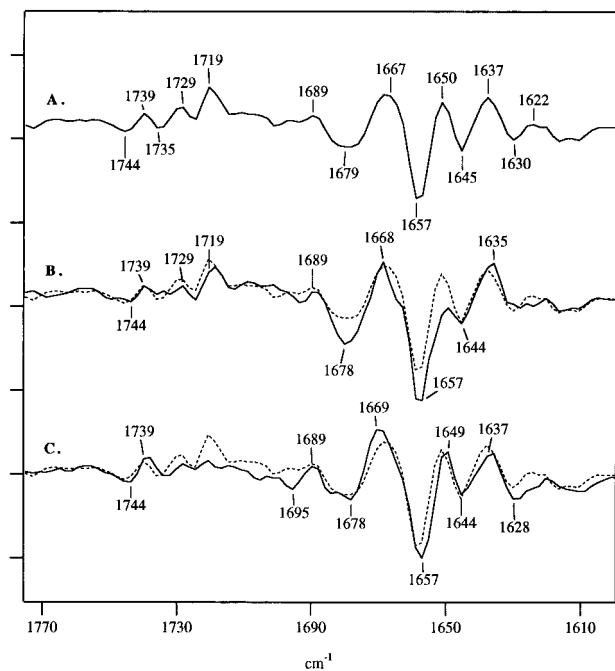


Figure 2. Light-minus-dark difference FT-IR spectra of plant photosystem II complexes obtained at (A) 200 K, (B) 130 K, and (C) 80 K. To facilitate comparison, spectrum A has been repeated in B and C as the dashed line. The tick marks on the y axis represent a ΔA of 1.0×10^{-3} . Spectral conditions are given in the Materials and Methods section.

± 0.01 chl⁺ per stable tyrosine radical D[•]. No EPR signals from the manganese cluster were observed at this illumination temperature. This result is in agreement with earlier characterizations of plant photosystem II membranes that contain low-potential cytochrome *b*-559.²⁴ Illumination of plant preparations at 200 K generated a chl⁺ radical in a stoichiometry of 0.39 ± 0.01 chl⁺ per stable tyrosine radical D[•].

In Figure 2, we present difference (light-minus-dark) infrared spectra that are associated with the generation of the multiline state (Figure 2A) and $g = 4.1$ state (Figure 2B) and with the photooxidation of chlorophyll (Figure 2C). The spectra are on the same absorbance scale and have been corrected for any small difference in the total amount of protein or pathlength (see Materials and Methods). Since these are difference spectra, unique vibrational modes of S₂ or chl⁺ will be positive lines, and unique vibrational modes of S₁ or chl will be negative lines. At all three temperatures, the terminal electron acceptor is the single-electron acceptor, Q_A.¹⁸ Therefore, each spectrum will also contain positive contributions from Q_A⁻ and negative contributions from Q_A. We assume that any spectral features due to quinone reduction have similar frequencies and intensities⁷ in all three difference spectra. Our discussion will center on spectral features from the donor side of photosystem II, which will be the unique vibrational lines observed at 130 and/or 200 K. Our future experiments will aim at an identification of the quinone vibrational difference spectrum through isotopic labeling. For a vibrational study of quinone reduction *in vitro*, see reference 26.

The spectra in Figure 2 show that spectral features in the 1680–1620 cm⁻¹ region are S₂ state dependent. In this region of the spectrum, contributions from the carbonyl stretching vibration, “amide I”, of the peptide backbone will dominate.²⁷ Intensities and frequencies in the amide I region of the spectrum

(26) Tripathi, G. N. R.; Schuler, R. H. *J. Phys. Chem.* **1987**, *91*, 5881–5885.

(27) Krimm, S.; Bandekar, J. In *Advances in Protein Chemistry*; Anfinsen, C. B., Edsall, J. T., Richards, F. M., Eds.; Academic Press: New York, 1986; Vol. 38, pp 181–364.

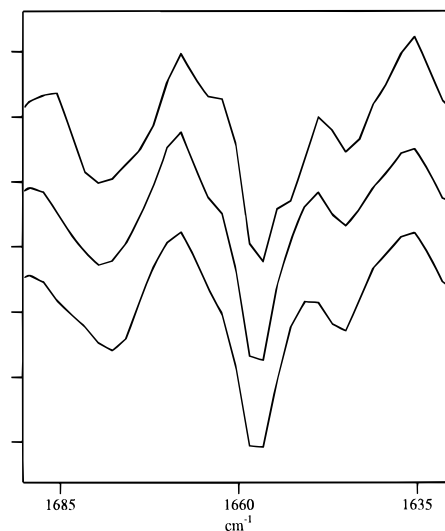


Figure 3. Replicate light-minus-dark difference FT-IR spectra of plant photosystem II complexes obtained at 130 K. The tick marks on the y axis represent a ΔA of 0.5×10^{-3} . Spectral conditions are given in the Materials and Methods section. Data correspond to individual light-minus-dark spectra before spectral averaging.

are influenced by the details of protein structure. For example, significant intensity in this region of the light-minus-dark difference spectrum may be associated with changes in secondary structure content or other changes in protein conformation upon charge separation. Alternatively, intensity in this region of the difference spectrum may be due to alterations in vibrational coupling constants; these changes could be caused by the generation of the positive and negative charges under illumination. Chlorophyll macrocycle vibrations may also contribute in this region,²⁸ as well as side chain vibrations from primary amide groups such as glutamine and asparagine.^{29,30}

Figure 2 shows that spectra obtained at 80, 130, and 200 K all exhibit both positive and negative lines in the 1680–1620 cm⁻¹ region of the difference spectrum. Interestingly, this region of the chl⁺-minus-chl spectrum (Figure 2C) and of the multiline S₂-minus-S₁ spectrum (Figure 2A) are similar. The small differences that do exist may be from an increased contribution of chlorophyll macrocycle vibrations.

However, the 1680–1620 cm⁻¹ region of the S₂ $g = 4.1$ -minus-S₁ spectrum (Figure 2B) differs from that of the other spectra, with increased intensity in negative lines at 1678 and 1657 cm⁻¹ and with decreased intensity in the positive line at 1650 cm⁻¹. There is also an additional shoulder at approximately 1664 cm⁻¹ in the 130 K difference spectrum. We tentatively assign these lines to amide I vibrational lines. It should be noted that these spectral features were reproducibly obtained in all data recorded at 130 K on these plant photosystem II preparations (for example, see Figure 3). Also, these features were not observed in samples with similar amide I absorbance upon illumination at 200 or 80 K (Figure 2, parts A and C).

Spectral features in the 1800–1700 cm⁻¹ spectral region will be considered next (Figures 2, 4 and 5). Chlorophyll oxidation is known to perturb the carbonyl vibrations of chlorophyll.²⁸ At 80 K (Figure 2C), the difference infrared spectrum should exhibit derivative-shaped features in the 1800–1600 cm⁻¹ spectral region. In Figure 2C, the most intense spectral feature

(28) Nabdryk, E.; Leonhard, M.; Mantle, W.; Breton, J. *Biochemistry* **1990**, *29*, 3242–3247.

(29) Flett, M. S. C. *Spectrochim. Acta* **1962**, *18*, 1537–1556.

(30) Bellamy, L. J. *The Infrared Spectra of Complex Molecules*; Chapman and Hall: London, 1980; Vol. 1, pp 183–202.

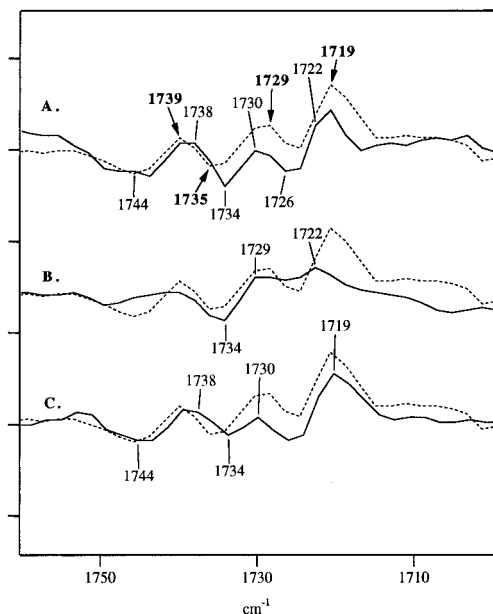


Figure 4. Light-minus-dark difference FT-IR spectra of photosystem II complexes obtained at 200 K. In A, B, and C, the dashed line shows the difference spectrum obtained on plant photosystem II complexes in $^1\text{H}_2\text{O}$ buffer, pH 6.0 (repeated from Figure 2A). In A, the solid line shows a spectrum obtained on plant photosystem II complexes in $^2\text{H}_2\text{O}$ buffer, pD 6.0. In B, the solid line shows the spectrum obtained on cyanobacterial photosystem II complexes, pH 6.5. In C, the solid line shows the spectrum obtained on manganese-depleted, non-oxygen-evolving plant photosystem II complexes, pH 6.0. No significant difference was observed in this spectral region when data were obtained on plant photosystem II complexes at pH 6.0 and pH 6.5. The tick marks on the y axis represent a ΔA of 0.55×10^{-3} . Spectral conditions are given in the Materials and Methods section.

is a derivative-shaped feature at 1744 (negative)/1739 (positive) cm^{-1} . We assign this spectral feature to the C=O of the 10 α -ester group of chlorophyll, in analogy to earlier assignments.^{28,31} Vibrational features from the C₉ keto group should also be observed; these may account for the low-intensity lines between 1730 and 1720 cm^{-1} .

Comparison of Figure 2A with Figure 2C reveals a new spectral feature associated with formation of the multiline S₂ state under continuous illumination. These spectra show that the photooxidation of the manganese cluster to form the multiline state is associated with the appearance of increased intensity in a derivative-shaped spectral feature at 1735/1729 cm^{-1} (see also expanded region in Figure 4A). At our current sensitivity, we can only say that this feature may be observed with lower intensity at 130 K (Figure 2B). Since illumination at 130 K results in a lower yield of the S₂ state,⁷ we cannot establish unequivocally if this spectral feature is also associated with the production of the S₂ $g = 4.1$ state.

The spectral feature at 1735/1729 cm^{-1} is also observed upon formation of the S₂ multiline state in cyanobacterial photosystem II (Figure 4B). However, this spectral feature is not observed with equal intensity upon illumination of manganese-depleted plant preparations at 200 K (Figure 4C). Remaining intensity in this region in manganese-depleted preparations is probably due to a spectral contribution from chlorophyll oxidation. Thus, the 1735/1729 cm^{-1} feature in Figures 2A and 4A,B does not arise solely from the oxidation of chlorophyll. Instead, this control experiment supports the association of this spectral feature with the production of the S₂ state.

(31) MacDonald, G. M.; Steenhuis, J. J.; Barry, B. A. *J. Biol. Chem.* **1995**, *270*, 8420–8428.

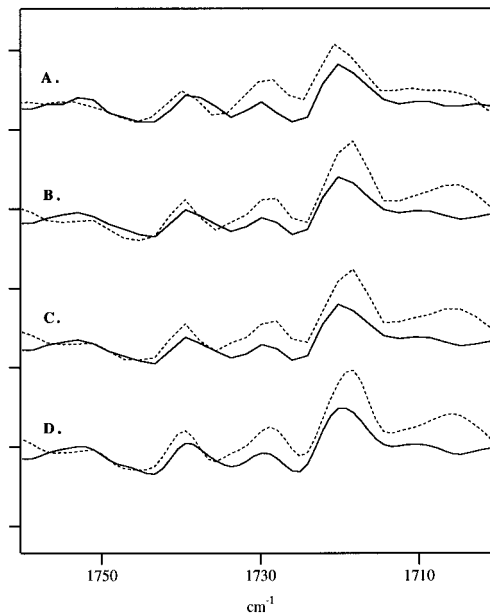


Figure 5. Light-minus-dark difference FT-IR spectra of photosystem II complexes obtained at 200 K. In each case the solid line shows data obtained on plant manganese-depleted photosystem II complexes, while the dashed line shows data obtained on plant manganese-containing photosystem II complexes. In A, data shown in the dotted line were obtained after averaging four (dashed line) and two (solid line) individual difference spectra. These data are repeated from Figure 4C. In B, C, and D, a single unaveraged difference spectrum is shown in both the dashed and solid lines. In C, a triangular apodization function, instead of a Happ–Ganzel function, was employed. In D, two levels of zero filling, instead of one level, were employed.

The 1735/1729 cm^{-1} feature is sensitive to $^2\text{H}_2\text{O}$ exchange (Figure 4A), as expected for the C=O vibration of hydrogen-bonded glutamic and aspartic acid residues.^{32–35} The downshifted derivative feature may be new negative and positive intensity at 1726/1722 cm^{-1} . A 7–9 cm^{-1} deuterium-induced downshift is reasonable for the C=O vibration of a carboxylic acid.^{32–35} The spectral effects of deuterium exchange are complicated by the fact that spectral features at 1719 cm^{-1} also decrease in intensity and downshift in $^2\text{H}_2\text{O}$ (Figure 4A, solid line).

Figure 5 shows that the infrared data were taken with appropriate spectral conditions so as to distinguish the small difference between manganese-depleted and manganese-containing samples in the 1735/1729 cm^{-1} region. In Figure 5A, difference spectra were averaged to give the final spectrum. These data were repeated from Figure 4C. In Figure 5B, we show that the spectral difference is observable before averaging. We also show that the spectral difference is still observed when a triangular apodization function is used, instead of a Happ–Ganzel function (Figure 5C), and when the interferograms have two levels of zero filling, instead of one (Figure 5D). Both the level of zero filling and the apodization function alter the resulting spectral line shapes, but the difference between manganese-containing and manganese-depleted spectra is still evident.

Discussion

Analysis of our S₂-minus-S₁ difference spectrum has led to two observations: (1) a $g = 4.1$ state dependent vibrational

(32) Haurie, M.; Novak, A. *J. Ch. Phys. Tome* **1965**, *62*, 137–157.

(33) Herman, R. C.; Hofstadter, R. *J. Chem. Phys.* **1939**, *7*, 460–464.

(34) Maeda, A.; Sasaki, J.; Shichida, Y.; Yoshizawa, T.; Chang, M.; Ni, B.; Needleman, R.; Lanyi, J. K. *Biochemistry* **1992**, *31*, 4684–4690.

(35) Weltner, W., Jr. *J. Am. Chem. Soc.* **1955**, *77*, 3941–3950.

“fingerprint” in the amide I region of the difference spectrum and (2) a new derivative-shaped feature, associated with the generation of the multiline form of the S_2 state, in the 1800–1700 cm^{-1} region.

Our first observation is that the amide I region of the spectrum shows a $g = 4.1$ state dependent vibrational signature. Our difference infrared data show that the amide I changes occurring upon charge separation in manganese-containing preparations at 80 and 200 K are similar to each other, in spite of the 120 K temperature difference. This result implies that temperature alterations alone do not cause significant secondary structural changes in photosystem II. At 130 K, the effect of charge separation on the vibrational spectrum of the peptide backbone is distinct from what is observed at 80 and 200 K. Thus, our data are consistent with the hypothesis^{7,8} that the generation of the S_2 $g = 4.1$ state is associated with a global protein conformation that is different from the structure of the protein that gives rise to the S_2 multiline state. We emphasize that we are generating a $g = 4.1$ signal which is produced with and without near-infrared illumination²³ of the sample.

We next consider the new derivative-shaped feature, associated with the generation of the multiline S_2 state. In the 1800–1700 cm^{-1} spectral region, carbonyl stretching vibrations of protonated carboxylic acid residues are typically observed.^{29,30} Thus, it is reasonable to consider such an assignment for the 1735/1729 cm^{-1} spectral feature. Both positive and negative lines exhibit a $^2\text{H}_2\text{O}$ exchange induced shift that supports this spectral assignment.^{32–35} There is considerable disagreement in the literature concerning the origin of such exchange-induced shifts of $\nu\text{C}=\text{O}$ in carboxylic acids. These shifts have sometimes been attributed to coupling between the OH and $\text{C}=\text{O}$ vibrational modes.³⁴ However, deuterium exchange in non-hydrogen-bonded carboxylic acid monomers in the vapor phase had no effect on $\nu\text{C}=\text{O}$.³⁵ Our reading of this literature causes us to favor the assignment of the 1735/1729 cm^{-1} spectral feature to one or more hydrogen-bonded carboxylic acid residues.

There is decreased intensity in the 1735/1729 cm^{-1} spectral feature upon illumination of manganese-containing preparations at 80 K and upon illumination of manganese-depleted preparations at 200 K. These results support the assignment of a component of this line to the S_2 -minus- S_1 state. The remaining component is probably due to chlorophyll oxidation. Moreover, a spectral feature with similar frequencies is observed upon illumination of cyanobacterial photosystem II preparations at 200 K. We conclude that the glutamic or aspartic acid residue giving rise to these vibrational lines is conserved in plants and in cyanobacteria.

A glutamic or aspartic acid residue may contribute to the difference infrared spectrum for two reasons: (1) charge separation causes a change in the intensity of the $\text{C}=\text{O}$ line or (2) charge separation causes a perturbation of the $\text{C}=\text{O}$ frequency. As an example of the first scenario, protonation of a carboxylate anion upon charge separation would give a positive spectral feature in the region from 1800 to 1700 cm^{-1} and two negative lines, corresponding to the asymmetric and symmetric stretching vibrations of the carboxylate, in the spectral region from 1620 to 1390 cm^{-1} .²⁹ As an example of the second scenario, any interaction that decreases the double-bond character of the $\text{C}=\text{O}$ bond or increases the basicity of the carbonyl oxygen serves to decrease the $\text{C}=\text{O}$ frequency.³⁰ Such a perturbation would give rise to a derivative-shape in the difference spectrum; this derivative-shape would have positive and negative components that are assignable to the same amino acid residue. Our interpretation of our spectra favors

this second possible explanation, since the positive 1729 cm^{-1} line is accompanied by a negative feature at 1735 cm^{-1} in both plant and cyanobacterial photosystem II. The glutamic/aspartic acid residue giving rise to this derivative-shaped vibrational feature must be solvent accessible, since both positive and negative lines decrease in intensity and downshift upon deuterium exchange.

What is the microscopic reason that the formation of the S_2 state perturbs the vibrational spectrum of this glutamic or aspartic acid residue? We will consider four possibilities: a change in pK_a , a change in hydrogen bonding, a change in dielectric constant, or a unidentate ligation to the metal cluster.

We consider the first possible explanation, which is that formation of S_2 perturbs the basicity of the glutamic or aspartic acid residue. Ignoring other effects, generation of an additional positive charge in the environment of a carboxylic acid residue would be expected to decrease the pK_a of such a residue. The positive charge should stabilize the anionic form. A linear correlation of $\nu\text{C}=\text{O}$ with pK_a has been observed for many different types of carboxylic acids.³⁰ In particular, the results of model studies on substituted benzoic acids are often used to calculate the magnitude of the expected pK_a shifts from an observed change in $\text{C}=\text{O}$ stretching frequency.³⁰ If we use this correlation, we predict a pK_a of 4.8 for a carboxylic acid with a $\nu\text{C}=\text{O}$ of 1729 cm^{-1} . Similarly, this correlation predicts a pK_a of 4.3 for a carboxylic acid residue with a $\nu\text{C}=\text{O}$ of 1735 cm^{-1} . The absolute values of these pK_a s are clearly incorrect, since this residue is protonated at pH 6.0 in both the S_1 and S_2 states. This error in absolute value is probably due to the importance of using long chain carboxylic acids as models for aspartic and glutamic acid residues in proteins, as recently discussed.³⁶ If we assume that the slope of the line is correct, even if the absolute values are not, we can calculate the change in pK_a . This calculation predicts that this residue undergoes a pK_a increase of approximately 0.5 unit upon formation of the S_2 multiline state from the S_1 state. Such an increase in pK_a cannot be simply explained by generation of additional positive charge on the metal cluster in the S_2 state. Therefore, we conclude that this vibrational feature is not simply due to an oxidation-induced change in basicity of this amino acid residue.

We next consider the second and third possible explanations. This carboxylic acid residue may be involved in a hydrogen-bonding network which undergoes a shift in equilibrium position upon formation of the S_2 multiline state. Introduction of hydrogen bonding through the use of solvent mixtures causes a downshift of $\text{C}=\text{O}$ frequency in carboxylic acids.³⁶ For example, $\nu\text{C}=\text{O}$ of the propionic acid monomer undergoes a downshift from 1740 to 1723 cm^{-1} on transfer from dioxane to trifluoroethanol.³⁶ Alternatively, the manganese site may be relatively anhydrous in the S_1 state and may admit water in the S_2 multiline state. Increases in dielectric constant are known to decrease $\text{C}=\text{O}$ frequencies.³⁶ Hydrogen bonds to water could also be formed; this would also downshift $\nu\text{C}=\text{O}$. It should be noted that ENDOR studies have disagreed in their assessment of the access of water to the manganese cluster in the S_2 state.^{37,38}

A fourth possible explanation for the observation of the 1735/1729 cm^{-1} spectral feature is that this feature arises from a hydrogen-bonded unidentate ligand to a manganese atom of the

(36) Diomaev, A. K.; Braiman, M. *J. Am. Chem. Soc.* **1995**, *117*, 10572–10574.

(37) Tang, X.-S.; Sivaraja, M.; Dismukes, G. C. *J. Am. Chem. Soc.* **1993**, *115*, 2382–2389.

(38) Kawamori, A.; Inui, T.; Ono, T.; Inoue, Y. *FEBS Lett.* **1989**, *254*, 219–224.

metal cluster. Such unidentate carboxylato metal ligands show relatively high frequency C=O vibrations, and oxidation of the metal would perturb the C=O frequency.³⁹ However, a ν C=O of 1740–1720 cm^{-1} is at the high end of observed frequencies for transition metal complexes in organic solvents.³⁹ Also, the observed downshift upon formation of S_2 from S_1 would need to be attributed to a decrease in O–M bond strength.⁴⁰ Such an interpretation seems to be in contradiction to expectations for oxidation of manganese from Mn(III) to Mn(IV).^{41,42}

After consideration of all these microscopic explanations, we favor the hypothesis that the 1735/1729 cm^{-1} spectral feature arises because of a change in hydrogen bonding or the dielectric constant upon formation of the multiline S_2 state. This residue may be in the vicinity of the manganese cluster, since it is affected by the formation of the S_2 state and since it undergoes facile deuterium exchange. However, more definitive evidence concerning the identity of this species must be obtained from site-directed mutagenesis experiments.

The effect of a change in dielectric constant or hydrogen bonding on the acidity of groups in the environment of the manganese cluster is of interest. An increase in the dielectric constant would be expected to decrease the $\text{p}K_a$, since it should stabilize the charged species. The effect of a change in hydrogen bonding on the $\text{p}K_a$ is harder to predict, since the effect depends on the manner in which the residue is hydrogen bonded and on the relative strengths of the hydrogen bonds in the protonated and unprotonated states.

Our difference infrared results differ from those obtained previously in a study of plant photosystem II membranes at

(39) Nakamoto, K. *Infrared and Raman Spectra of Inorganic and Coordination Compounds*; John Wiley & Sons: New York, 1986; pp 191–374.

(40) Greenwood, N. N. *Spectroscopic Properties of Inorganic and Organometallic Compounds*; The Chemical Society: London, 1968; pp 199–206.

(41) Larson, E. J.; Pecoraro, V. L. in *Manganese Redox Enzymes*; Pecoraro, V., Ed.; VCH Publishers: New York, 1992; pp 1–28.

(42) Sauer, K.; Yachandra, V. K.; Britt, R. D.; Klein, M. P. In *Manganese Redox Enzymes*; Pecoraro, V., Ed.; VCH Publishers: New York, 1992; pp 141–176.

temperatures from 80 to 240 K.^{43,44} The origin of spectral differences between our data and the data of Noguchi is under investigation.

Our results indicate that difference infrared spectroscopy is a new method with which to study the mechanism of water oxidation. In particular, infrared spectroscopy provides a technique with which amino acid residues in the vicinity of or ligating to the manganese cluster can be identified. Our data support the conclusion that formation of the multiline form of the S_2 state perturbs the vibrational spectrum of a glutamic or aspartic acid residue. The D1 and D2 polypeptides are thought to provide at least some of the amino acids that are in the vicinity of or ligating to the manganese cluster. Examination of regions predicted to lie close to the water-oxidizing site shows many carboxylic acid residues.^{45–47} Furthermore, site-directed mutagenesis studies have shown carboxylic acid residues to be important in the assembly or stability of the manganese cluster.^{48–50} Future experiments will aim to assign vibrational features to individual amino acid residues in the photosystem II reaction center through the use of site-directed mutagenesis.

Acknowledgment. We thank Dr. Marion Thurnauer for use of the Varian E9 EPR spectrometer at Argonne National Laboratory. This work was supported by NSF MCB 94-18164. J.J.S. was partially supported by a National Institutes of Health Training Grant award, GM08277.

JA961691V

(43) Noguchi, T.; Ono, T.-a.; Inoue, Y. *Biochim. Biophys. Acta* **1993**, *1143*, 333–336.

(44) Noguchi, T.; Ono, T.-a.; Inoue, Y. *Biochim. Biophys. Acta* **1995**, *1228*, 189–200.

(45) Trebst, A. Z. *Naturforsch.* **1986**, *41c*, 240–245.

(46) Svensson, B.; Vass, I.; Cedergren, E.; Styring, S. *EMBO J.* **1990**, *7*, 2051–2059.

(47) Ruffle, S. V.; Donnelly, D.; Blundell, T. L.; Nugent, J. H. A. *Photosynth. Res.* **1992**, *34*, 287–300.

(48) Vermaas, W.; Charite, J.; Shen, G. *Biochemistry* **1990**, *29*, 5325–5332.

(49) Boerner, R. J.; Nguyen, A. P.; Barry, B. A.; Debus, R. J. *Biochemistry* **1992**, *31*, 6660–6672.

(50) Nixon, P. J.; Diner, B. A. *Biochemistry* **1992**, *31*, 942–948.